geotechnics

MDPI

Article

Finer Measurement Scales for Induced Hydrophobicity Using the Water Droplet Penetration Test

Max Veneris and Arvin Farid *

College of Engineering, Boise State University, Boise, ID 83725, USA; maxveneris@u.boisestate.edu
* Correspondence: arvinfarid@boisestate.edu

Abstract: The Water Droplet Penetration Test (WDPT) is commonly used in most soil water repellency (SWR) research and is particularly prominent in field studies after wildfire events. Suppose a water droplet does not infiltrate the soil within the first five seconds. This soil is considered to contain some degree of water repellency, classified by the overall penetration time. Our results show an inflection point in the plot of the height of a droplet vs. droplet penetration time during a WDPT trial. This inflection point is indicative of a combination of two possible flow patterns influencing droplet penetration, one governing and the other—caused by particle lift—drastically impeding the infiltration rate. The reorganization of the intrinsic particle lift at the air–water interface leads to contact angles hindering the expected penetration, delaying the expected infiltration rate to degrees larger than a continuously flat porous hydrophobic surface would. The particle lift creates an instability that can create two competing regimes, leading to two sets of water droplet penetration times. The similarity among sorptivity values for coarse grains at higher hydrophobicity levels, medium grains at intermediate hydrophobicity levels, and fine grains at lower hydrophobicity levels suggests that interpretation of the WDPT needs to be adjusted based on grain size.

Keywords: hydrophobicity; soil water repellency; SWR; wildfires; burned soil; sorptivity; infiltration; WDPT

check for updates

Citation: Veneris, M.; Farid, A. Finer Measurement Scales for Induced Hydrophobicity Using the Water Droplet Penetration Test. *Geotechnics* **2024**, *4*, 581–603. https://doi.org/10.3390/geotechnics4020032

Received: 21 April 2024
Revised: 4 June 2024
Accepted: 7 June 2024
Published: 11 June 2024

Copyright: © 2024 by the authors. Licensee MDPI, Basel, Switzerland. This article is an open access article distributed under the terms and conditions of the Creative Commons Attribution (CC BY) license (https://creativecommons.org/licenses/by/4.0/).

1. Introduction

Soil hydrophobicity, a property of soils that repel water, is commonly seen in the upper soil layers. Soil hydrophobicity can either naturally exist— typically due to the type of vegetation—or occur after wildfires [1–3]. Wildfires can cause soil hydrophobicity via changing the surface chemistry of soil particles caused by particles coated with condensates of volatilized, naturally occurring organic hydrophobic compounds during a high-heat event [1,2]. This change in soil properties directly affects water infiltration rates and, in turn, soil erosion and revegetation rates [1,2]. These effects can be extrapolated into and observed in the field in terms of revegetation rates using available free and nutrient water, slope stability and raindrop impact erosion, and overall soil structure [1–3].

Wildfires can also have other varying but well-documented effects on soil properties. These effects can be linked to soil type, prominent vegetation, soil moisture content, and burn severity. Burn severity as classified by the United States Department of Agriculture Burned Area Emergency Response, BAER, details differences between low-, moderate-, and high-severity burns in soils. The key differences listed include color changes, degree of incineration of organics, loss of aggregate stability, and water repellency [4,5].

While soil hydrophobicity is well documented and is a key area of post-fire soil research and restoration, the tools and techniques utilized for hydrophobicity classification are still developing. The Water Droplet Penetration Test, WDPT, was first established by Letey in 1969 [6]. This test is one of the most commonly used ways to measure soil water repellence (SWR) in the majority of field research. This test is primarily used as a field test and is typically only a reference point, as no specialized equipment is required. The majority

of field SWR studies utilize the WDPT due to its simplicity and ease of use outside of the laboratory. The subjectivity of the WDPT has also led to the inclusion of other procedures, such as the Molarity Ethanol Drop (MED) test, Critical Surface Tension (CST), the Mini-disk Infiltrometer, and the measurement of contact angle [5,7–9]. Other tests are also emerging into the SWR research area to better define hydrophobicity in a larger capacity as a soil mechanics property and correlate and collate it to other properties. These properties include sorptivity, capillary action, hydraulic conductivity, and regimes governing the development of erosion, to name a few [8–10]. Even though newer test methods are improving the accuracy of and removing subjectivity from SWR classification, the WDPT is still commonly utilized for SWR classification due to its simplicity and commonality.

While common in research and practice, the limitations of the WDPT include its accuracy due to the exclusion of particle lift, correlation to soil properties other than SWR, and correction for aspects such as capillary action, evaporation, and other complex mechanisms common in heterogeneous soils. The WDPT does not account for the soil grain size, soil type, or any other variable than time. The objective of this research is to better understand the impact of grain size and improve the resolution and accuracy of the WDPT by adding an additional dimension to the established method. This would further enable the addition of needed criteria for the calibration of the WDPT in the field, considering its popularity.

The subjectivity of the WDPT is well-known, and intent is known to be a primitive methodology for field use. The intent of this work is to highlight the components of the method that cause subjectivity and identify factors that influence the WDPT results. The intent of this paper is not to deem the method obsolete nor prove the subjectiveness beyond the acknowledgement that it exists.

2. Background

SWR tendencies in soil are typically considered to be most severe when the strata are at low in situ moisture levels. Soils have also been observed—even at high levels of SWR—to show hydrophilic characteristics when they are later wetted to near or above the soil saturation point [11]. Some hydrophobic soils can show hydrophilic tendencies when 12–25% moisture by weight is added to the sample [12]. This has been observed by other researchers at varying percentages depending on the soil type, with soils only returning to hydrophobic conditions after long drying times [13,14].

Research by Pardini et al. [15] showed that the incorporation of water-repellent humic compounds into the soil profile can be induced by *E. arborea* (tree heath). This process contributes to the formation of organo-mineral complexes through a continuous cycle of mineralization and humification. Furthermore, Carballeira [16] and Ammar et al. [17] discovered certain phenolic compounds in the tissues of *E. australis* and the soils associated with it, which can lead to significant water repellency [14].

Moreover, the development of a substantial water-repellent layer on the soil surface can be facilitated by the low rate of litter mineralization provided by heath [18]. It is also known that specific types of vegetation can naturally induce hydrophobicity in soils. For instance, evergreen trees like coniferous and eucalyptus have been well documented for their potential to cause severe hydrophobicity. This is due to the discharge of resins, waxes, and other organic substances from their tissues, which then migrate to the soil surface [2].

As mentioned, soil water repellency is caused by hydrophobic coatings of a primarily organic nature that can occur naturally. Soil water repellency can be a naturally occurring phenomenon with or without wildfires. While the USDA Field Guide for Mapping Soil Burn Severity—used for burned soil classification—states that SWR is commonly present only in the upper one inch (1 inch.) of the scorched surface; this could be skewed due to the increased erosion potential of the top hydrophobic layer. Soil hydrophobicity has, however, been observed at varying depths from the ground surface. As described in the USDA Field Guide and in other works, common fire-induced hydrophobicity is seen at depths between 2 and 10 cm [1,19,20].

The true depth of fire-induced hydrophobicity is primarily a function of in situ moisture content, soil mechanical properties, organic content, and applied temperature [12,21].

On the contrary, on naturally hydrophobic soils, a wildfire may destroy the top layers' SWR and render it hydrophilic due to re-volatilization of the hydrophobic particle coatings. In these cases, the lower strata still maintain the ability to become hydrophobic due to the processes stated above. Excess heat is the primary instrument for re-volatilizing the organic compounds primarily responsible for hydrophobicity [5,10].

Droplets on a hydrophobic surface ball up and form marble-like shapes, commonly causing soil particles to lift and coat the 'marble.' The speeds of the particle lift and resulting marble coverage are a function of the degree of hydrophobicity, grain size, liquid in intermolecular forces, and other contaminates present in the soil. This process is evaporatively driven and directly relates to the free energy at the contact points between the soil, water, and atmosphere [8]. The contact angle of the water against the soil is a direct response to the interface tension between the liquid and solids and can be used to determine wettability. Molecular dynamic models have been successfully applied and shown to be valid for soils [22]. However, unlike the wetting/drying angles measured on a flat glass surface, even consistently induced levels of hydrophobicity can still appear as different wettability and varying contact angles due to grain structure, surface roughness, and temperature.

Another phenomenon observed during droplet penetration into soil is particle lift. Particle lift can be described as individual particles ascending the water marble as infiltration occurs. Lifted particles have been observed to have both hydrophobic and hydrophilic surfaces, although the outer layer and/or portions of those particles in burned soils are composed of entirely hydrophobic sections. According to Young's Law, the surface-energy change is always negative and favorable for soil particles to attach themselves to the air–water interface. As the droplet collapses due to infiltration, particles will continue to compete for a location at this lower free-energy interface. When hydrophobic particles are lifted by the droplet, they will orientate themselves in a way that leads to the exclusion of hydrophobic—or the most hydrophobic—portions of the particle to any availability possible. This brings a rough surface to the previously smooth and pure water droplet [8,9]. The inconsistency of hydrophobic coating is consistent with Doerr's observations of a segregated structure, although he hypothesized that additional heat could encourage the even distribution of the coating [18].

Typically, fire-induced soil hydrophobicity has a rapid onset after a fire event due to the solidification of the vaporized organic compounds. While the immediate effects can be severe, the temporal length of the repellency is dependent upon several factors, including environmental conditions, soil type, moisture content, and erosion. In some situations, such as in wildfires in *Pinus ponderosa* forests in Front Range, Colorado, many highly repellent areas were observed, although the same locations showed significantly deteriorated SWR severity levels just three months later. Other areas tested 22 months later showed even further deterioration of the water repellency layer [12]. Simultaneously, burn sites of Ponderosa forests in the Oregon Cascades, when observed six years after a fire event by Dyrness circa 1975 [23], and in Arizona four years later by Campbell et al. [24], manifested high levels of SWR. Others who performed research on the persistence of SWR faced varying results appearing to be highly dependent on various environmental factors [2,6,12].

3. Methodology

To create a controlled environment, various hydrophobic specimens of commercially produced sands were prepared utilizing a surrogate hydrophobicity-inducing product at varying rates of dilution in deionized water. The utilized sand consisted of an angular clean aggregate that was sieved to create three relatively uniform groups of samples—the first one with sizes of 0.6–2.0 mm, hereafter referred to as the coarse samples; 0.3–0.6 mm, referred to as the medium samples; and 0.075–0.3 mm material, referred to as the fine samples.

The surrogate product used was Nikwax Wax Cotto–Proof TM. This product is a synthetic, water-soluble, and highly liquid-repellent elastomer. The surrogate was diluted to concentrations of 0.6%, 0.7%, and 0.8% by volume in water. All concentrations stated within this paper will refer to diluted surrogate concentrations as a means of inducing a level of hydrophobicity. Then, 6 mL of each diluted solution was thoroughly mixed into 8.0–10.0 g of each sand sample to create testing specimens of three grain sizes (fine, medium, and coarse), with three dilution rates (0.6%, 0.7%, and 0.8%) each. The specimens were then dried in a low-temperature oven at 43 °C until a constant mass was achieved, cooled, and then thoroughly disturbed. The medium and fine specimens had a clear residual material that initially made the particles stick together and had to be knocked apart. The fine sample also had a thin top layer, light in color, with a brittle surface and homogeneous underlayer. This surface layer was broken apart and thoroughly mixed with the remainder of the sample. The diluted hydrophobicity-inducing surrogate liquid was added to the soil samples in variations of 0.2–0.8% by mass. This percentage range is consistent with other findings of the additional mass required to produce SWR of natural soils in the literature [18].

Soil specimens were then poured into a conical shape using dry pluviation, allowing the material to freely flow from the container to the plate from a height of approximately 4 cm. The top of every sample was then struck off to maintain a constant sample depth of 6 mm above the glass. Water droplets were placed on top of the sand specimens, three to four at a time, and digital images were taken. The droplets were placed with a pipette and placed from 0 to 2 mm above the sand bed. The camera used was a Canon camera, Model EOS Rebel T4i. The camera obtained a video of the entire infiltration process; then, frames were exported from the video when the droplets had dropped in height by more than 0.1 mm or five minutes, depending on which occurred first. Figure 1 shows the experimental setup utilized for WDPT documentation. The droplet heights and contact angles were manually measured and documented through the full infiltration time from the frames exported. The heights were recorded to the nearest 0.1 mm and measured from the base of the sand to the highest point of the water marble (shown in Figures 2–4). Both right- and left-hand contact angles were recorded, and the average was reported (shown in Figures 5–7 against time).



Figure 1. Experimental setup for imaging WDPTs, including height and contact angle.

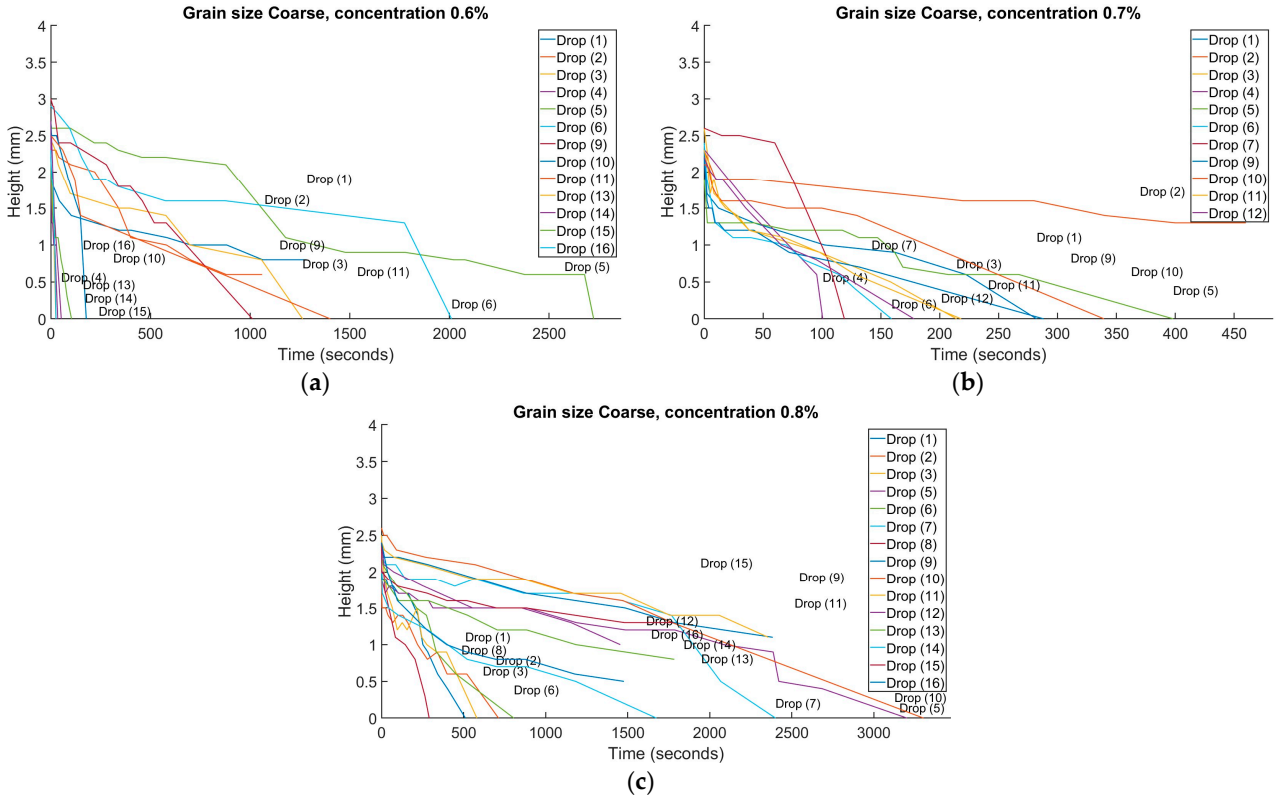


Figure 2. Water Droplet Penetration Test results (i.e., height vs. time) for coarse-grained soil for hydrophobicity-inducing surrogate dilutions of (**a**) 0.6%, (**b**) 0.7%, and (**c**) 0.8%.

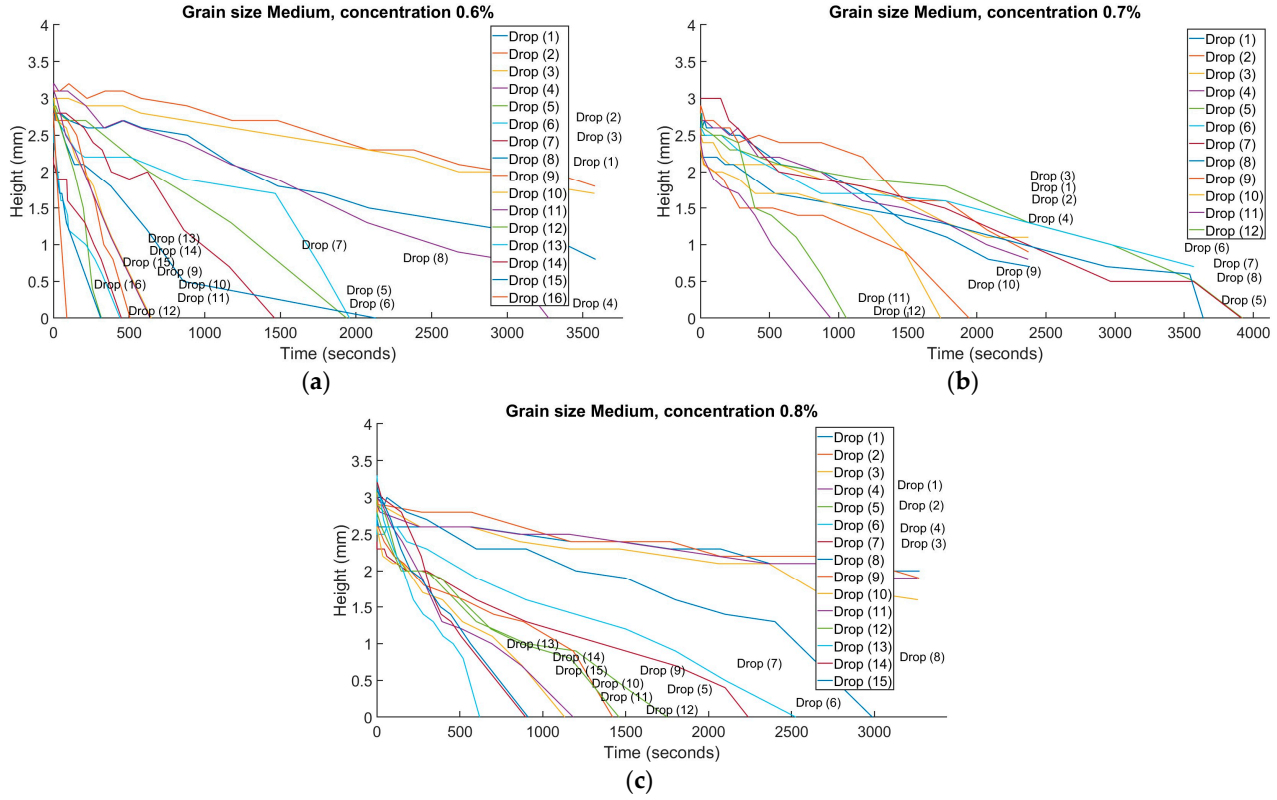


Figure 3. Water Droplet Penetration Test results (i.e., height vs. time) for medium-grained soil for hydrophobicity-inducing surrogate dilutions of (**a**) 0.6%, (**b**) 0.7%, and (**c**) 0.8%.

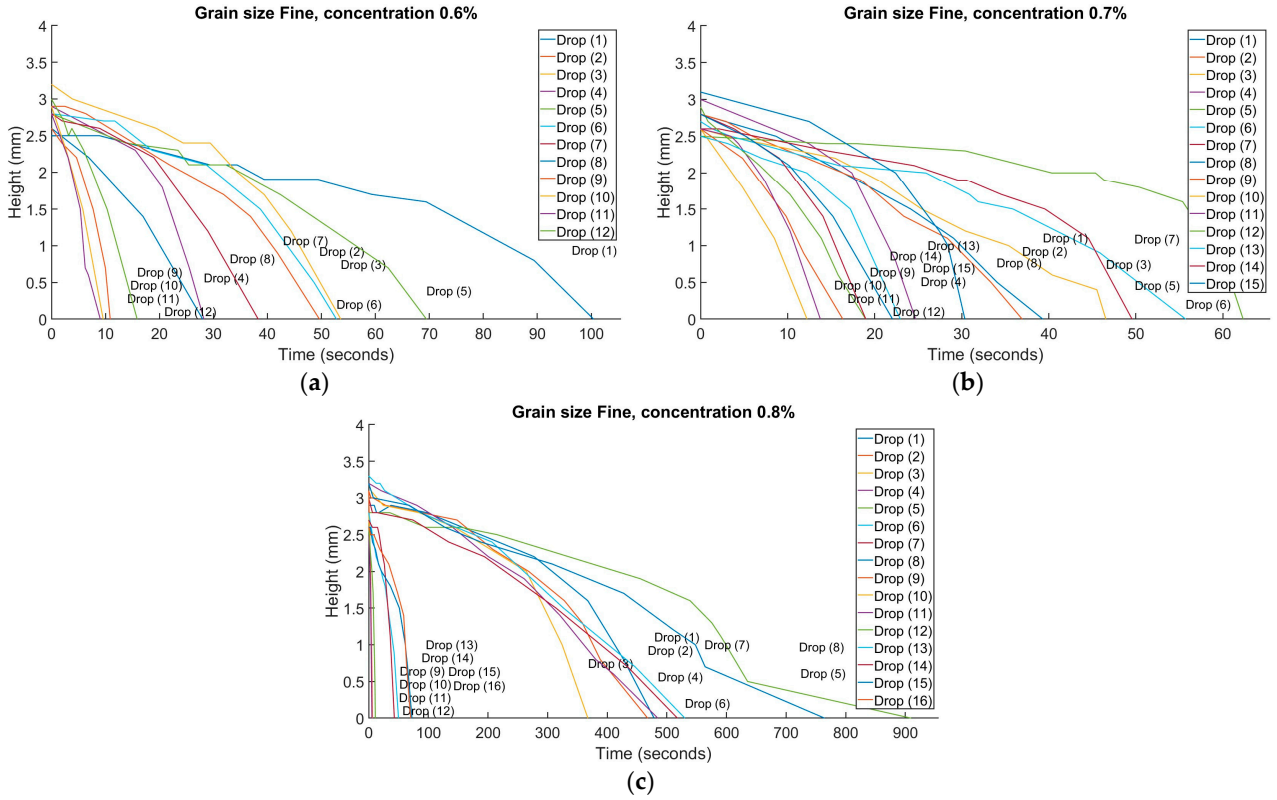


Figure 4. Water Droplet Penetration Test results (i.e., height vs. time) for fine-grained soil for hydrophobicity-inducing surrogate dilutions of (**a**) 0.6%, (**b**) 0.7%, and (**c**) 0.8%.

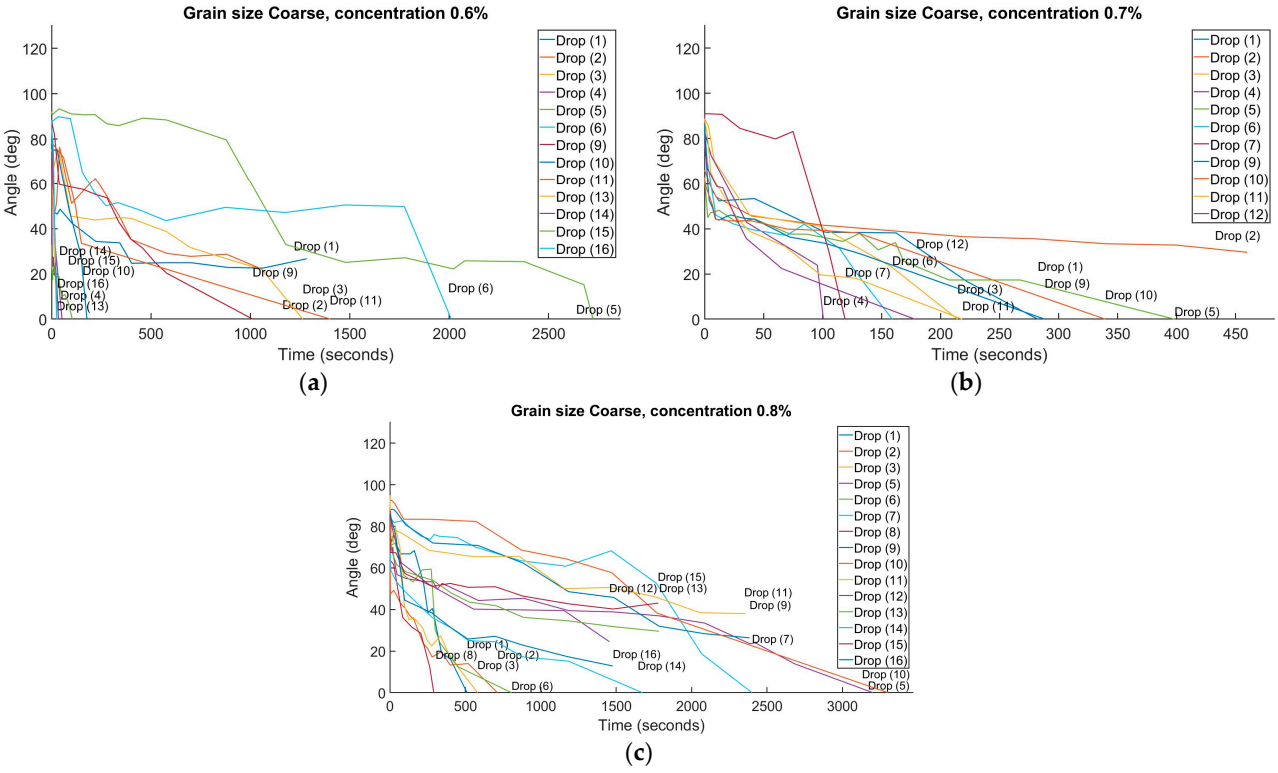


Figure 5. Changes in the average contact angle of the water droplet over time for coarse-grained soil for hydrophobicity-inducing surrogate dilutions of (**a**) 0.6%, (**b**) 0.7%, and (**c**) 0.8.

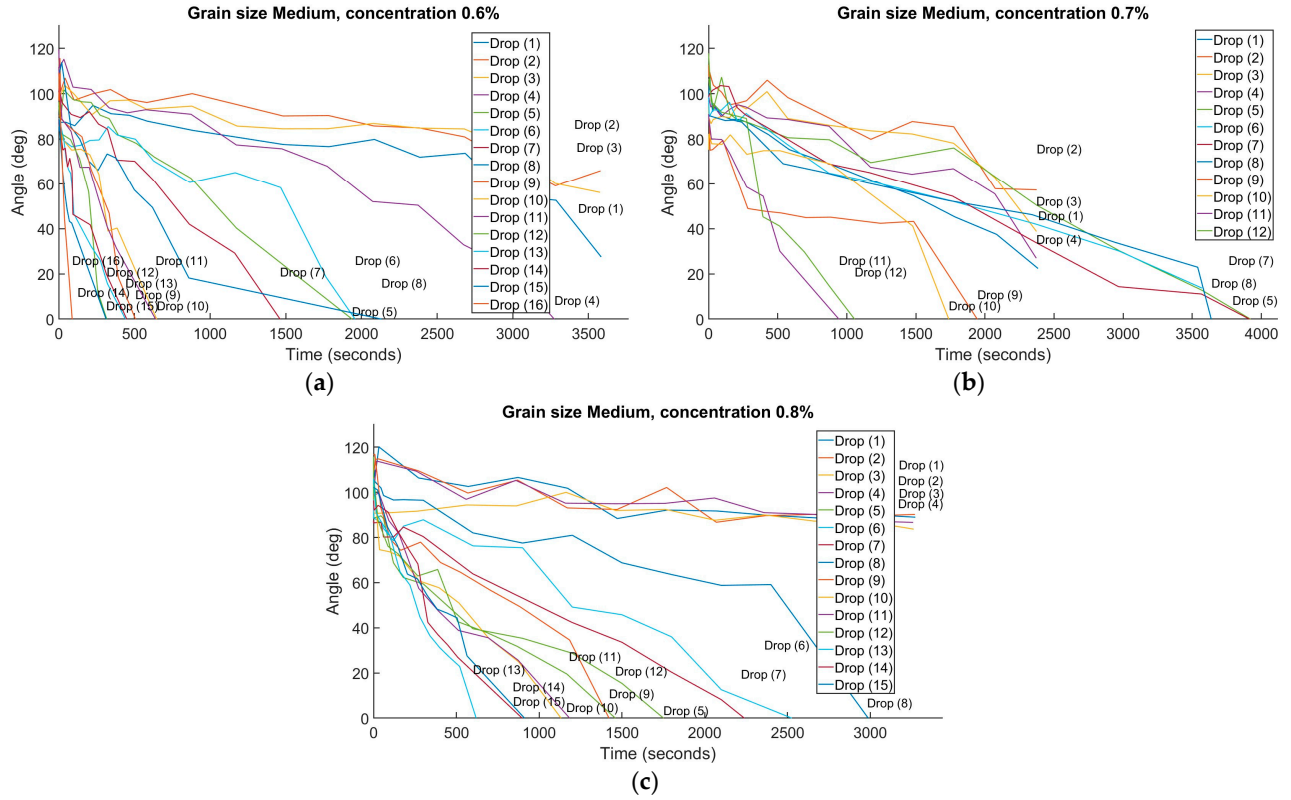


Figure 6. Changes in the average contact angle of the water droplet over time for medium-grained soil for hydrophobicity-inducing surrogate dilutions of (**a**) 0.6%, (**b**) 0.7%, and (**c**) 0.8%.

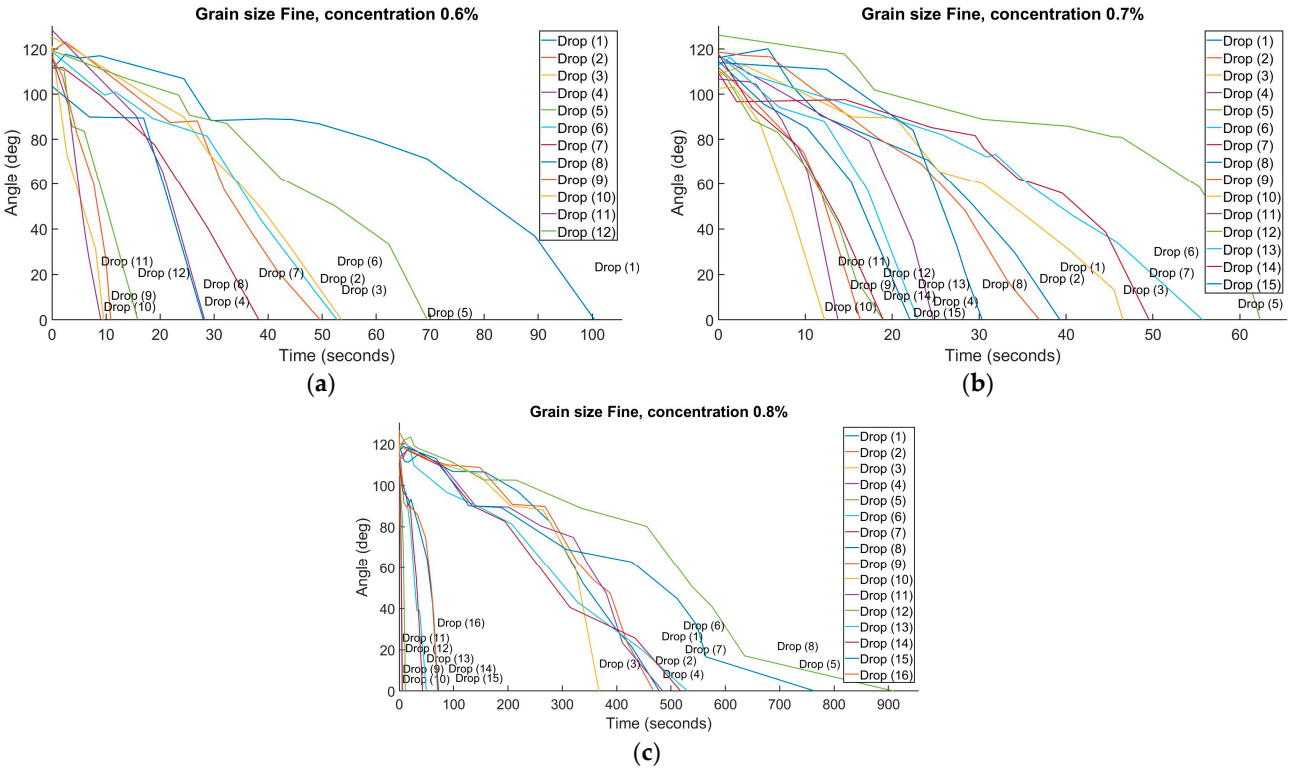


Figure 7. Changes in the average contact angle of the water droplet over time for fine-grained soil for hydrophobicity-inducing surrogate dilutions of (**a**) 0.6%, (**b**) 0.7%, and (**c**) 0.8%.

A series of WDPT trials were conducted on the sand specimens prepared as mentioned. Typically, four water droplets could be placed on a single pile of prepared sand to ensure no interference by the infiltration paths or due to water diffusion. WDPT trials were normally monitored in sets of four and typically included a total of 16 drops as described in Section 4.1, unless it was determined that a test trial was to be deemed invalid. These reasons would include water droplets being placed too close and disturbance of the test procedure apparatus (e.g., vibrations, large movements of the water droplet on the pile, or any other occurrence that would interfere with results). Experimentation was conducted in an open-air laboratory environment with controlled low but unmonitored levels of humidity and air movement at an approximately 22 °C ambient temperature.

Test times were determined to be somewhat subjective, as the definition of full penetration, as discussed in other literature, was assumed to be comprehensive. The definition of full infiltration likely was intended to be utilized in the field and observed with the naked eye. Digital imagery enabled visual determination of the upward movement of particles in capillary action, and further investigation showed water droplets coated with soil particles appeared to be penetrated but were still intact, albeit sunken within the soil surface.

The end times reported here are the times at which no more movement could be discerned of the water marble or grain movement from the camera's angle. Grain movement near the end of a penetration time was due to the capillary action of the water climbing up, lifting, or otherwise supporting particles above the original dry and undisturbed plane. Inconsistencies in the WDPT have been well established [4,23,25], as has the coating of hydrophobic material around soil particles [18]. The data collected appear to be segregated into two or three categories governed by different 'regimes' rather than outliers or chaotic patterns. Studying this observed inconsistency and finding the factors controlling those regimes and regime shifts causing instability are the objectives of this research.

Some researchers treated and sterilized their sand samples with chemicals, such as hydrogen chloride or hydrogen peroxide, to neutralize and remove impurities or contaminates [1,8,10]. The sand used in this experiment was untreated, commercially available clean aggregate, and was untreated in this experiment.

The Philip Infiltration equation was used to compute sorptivity based on the WDPT. Philip's infiltration equation is a simplified model showing that complex infiltration can be accurately analyzed utilizing a rapidly converging power series as the square root of time. The first two terms of the series can be understood as total infiltration and time, t, representing the time since ponding [26].

$$I = S.t^{(1/2)} + A.t \quad (1)$$

where I is the cumulative infiltration (cm); S is sorptivity ($1/\sqrt{s}$); t is time (s); A is a constant and a function of hydraulic conductivity, moisture, and other soil properties according to Shillito [9].

The Philip Infiltration equation can be rewritten to solve for sorptivity [26,27].

$$S = (I - A.t)/\sqrt{t} \quad (2)$$

The primary dependent variable, I, is the cumulative infiltration distance at any given time, t, and is considered to be the initial drop height in this experiment. The time, t, is in seconds and is the WDPT time. Sorptivity values were only calculated for drops where the full WDPT time was measured; no WDPT times were approximated for calculation purposes.

The A value in the Philip Infiltration equation (Equations (1) and (2)) is a constant, reflecting the steady-state rate at long times. Parameter A has a level of uncertainty in the estimation, and the equation could be inappropriate for long-term experiments (e.g., estimation of the Philip infiltration parameters from rainfall and long-term seepage). While this value has been correlated empirically to steady infiltration rates, a higher degree of uncertainty comes with the estimation of the A value for water droplet penetration [27].

The unsaturated hydraulic conductivity of dry soils, at the beginning of water droplet testing, is considerably smaller than the saturated values and close to zero. A is heavily dependent on hydraulic conductivity and steady-state flow. Hence, the value for A can be negated to zero during the initial stages of infiltration based on a Two-Term model [26] when the soil is almost dry. Other researchers [26–28] confirmed that it is reasonable to consider steady-state inputs negligible during this unsaturated flow state as long as initial conditions are dry. As a result, the model suggests that during the initial stages of infiltration (i.e., when time is small) the first term relating to sorptivity dominates the process. In this stage, vertical infiltration proceeds at the same rate as absorption or horizontal infiltration.

To calculate sorptivity, three parameters, i.e., the water droplet volume, infiltration area, and time of infiltration, were utilized. The radius of the drop was established by manually measuring the water droplets' size at the initial placement and adjusting for bulging by averaging the difference between the assumed spherical and the flat-bottom elliptical droplet shape, utilizing the droplet height and width. Once an initial droplet volume had been estimated based on the droplet height at the first recorded measurement, a constant value for the estimated infiltration area of a circular 4.5 mm diameter sphere was utilized for cumulative infiltration. Infiltration time in seconds was then plugged into the modified equation (Equation (2)) for unsaturated flow to calculate sorptivity.

As mentioned, the initial drop volume was an approximate value based on the height of the droplet. The average drop diameter was measured directly at contact when the overall shape appeared to be spherical, and a difference of 0.834 mL was established as the difference between the approximated spherical diameter and the initial droplet height. This value was added to each droplet height, and the volume was calculated and then divided by the approximated infiltration area. The infiltration area was calculated in the same fashion and was approximated to be that of a circle with a 4.5 mm diameter.

Particle lift was qualitatively observed in each droplet from the digital images. Particle lift does not have a qualitative analytical method that is currently established or widely used. Numerical values of 0 to 4 were given to each droplet at the initial stabilization of the droplet after placement, less than 0.1 s, and then after the droplet height had shrunk due to infiltration by 0.5 mm. The values of 0 to 4 were based on a qualitative assessment of the particle cover of the visible face of the droplet and can be equated to approximately 0, 25, 50, 75, and 100% coverage $\pm$ 12.5%. Due to this method's subjectivity and qualitative nature, the following categories were substituted for transparency: None, Low, Mild, High, and Full.

The infiltration tests produced results that, when compared with the calculated sorptivity values and characterizations of the penetration plots, led to the identification of two infiltration patterns. These patterns represent two groups that can be designated within an infiltration regime. The WDPT of these groups depends on whether rapid particle lift occurs early in the infiltration process. To distinguish these groups, it is necessary to quantify the particle lift and correlate it with the rate of change in the water droplet penetration over time.

4. Results and Discussion

4.1. Summary of Results

The following section includes the results from the Water Droplet Penetration Test, digital imaging, and sorptivity calculations.

WDPT times varied significantly, even when concentrations of the hydrophobicity-inducing product and grain size were maintained consistently. Figures 2–4 show the penetration of the water droplet over time (i.e., height vs. time) for three grain sizes (coarse, medium, and fine). Figures for each grain size are also shown for the three dilution levels of the hydrophobicity-inducing surrogate.

Figures 5–7 show the change in the average contact angles of each water droplet over time for three grain sizes (coarse, medium, and fine). Figures for each grain size are also shown for three dilution levels of the hydrophobicity-inducing surrogate.

Some drops did not fully penetrate the soils rendered hydrophobic. The time to full penetration was extrapolated to find penetration time using polynomial fit data. Those extrapolated values are shown in Table 1. This table shows the overall penetration time ranges for all results separated by grain size and concentration.

Table 1. WDPT time ranges (s).

Concentration (%) Grain Size	0.6%	0.7%	0.8%
Coarse	25–180, 1000–1450, 2000	100–400, 700	290–800, 1700, 2400–3200
Medium	90–650, 1450–2150, 3200–3700	940–1050, 1740–1950, 3600–4200	620–910, 1130–3000, 4600–5800
Fine	8–100	12–65	5–70, 360–590, 760–890

The results of Figures 2–4 in trials that reached full penetration were then used to calculate the sorptivity. Figure 8 shows the average sorptivity for each grain size at three surrogate dilution levels. As seen in the example in Figure 9 for a coarse-grained sample at 0.6% surrogate dilution, the averages of Figure 8 have large error bars/standard deviations due to the aforementioned particle lift only occurring in some cases, not all.

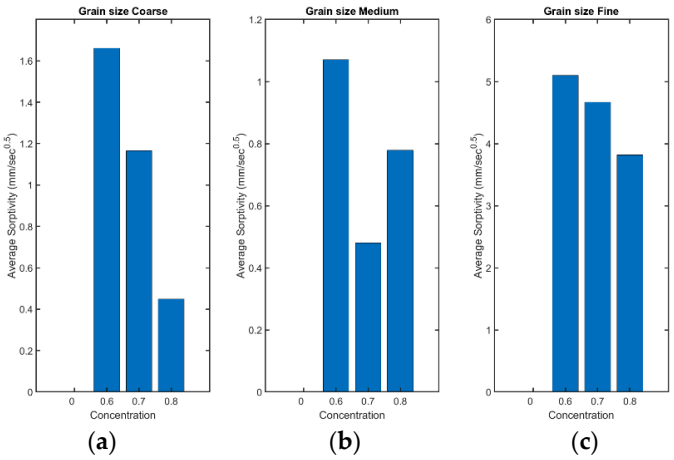


Figure 8. Average sorptivity values across grain size and surrogate dilution of: (**a**) coarse, (**b**) medium, and (**c**) fine grained samples.

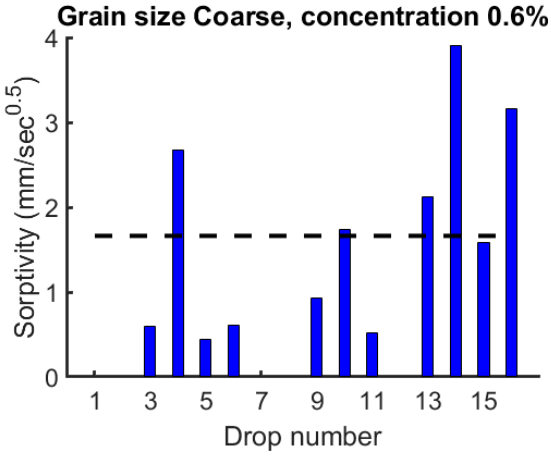


Figure 9. Example of sorptivity calculated for 16 drops on coarse-grained soil at 0.6% dilution. The black dashed line represents the average value shown in Figure 8.

The number, n, and standard deviations, s, in (mm/s$^{0.5}$) for Figure 8a are n = 11 and s = 1.133 for 0.6% dilution, n = 10 and s = 0.0.410 for 0.7% dilution, and n = 9 and s = 0.138 for 0.8% dilution. The values of n and s for Figure 8b are n = 13 and s = 0.560 for 0.6% dilution, n = 7 and s = 0.164 for 0.7% dilution, and n = 11 and s = 0.316 for 0.8% dilution. For Figure 8c, the n and s values are n = 12 and s = 2.091 for 0.6% dilution, n = 15 and s = 1.267 for 0.7% dilution, and n = 16 and s = 3.557 for 0.8% dilution.

As seen in Figure 9, there is a large variation among the sorptivity calculated for the 16 drops above. This chaotic pattern exists, to some degree, for all other cases. There is a separation into two distinct ranges of sorptivity values. This difference appears to occur when there is a considerable amount of particle lift. When a hydrophobic particle is lifted, air pockets form underneath the particle, leading to slower unsaturated flow; i.e., new dry surfaces are exposed and need to be overcome, hindering the furtherance of wetting and slowing the infiltration. In other words, where there is considerable particle lift, the slope (i.e., time rate of penetration) in Figures 2–7 will be smaller, and penetration slows. The intensity of this impact varies for various grain sizes at various degrees of hydrophobicity rendered by various surrogate dilution levels.

Hence, the first step is to quantify particle lift. It should be noted that, while untested here, laboratory observations showed the inside of the droplet to remain transparent, and the darkening seen in the droplets was due to a surface cover. Thus, it seems that in these experiments, particles are attracted to the water–air interface (droplet surface) and are not fully suspended inside the droplet. Hence, the particle cover causing opacity in digital images is not referred to as turbidity and is just qualitatively used to distinguish degrees of particle lift. Figure 10 shows a digital image marking what is considered various levels of particle lift.



Figure 10. From left to right, droplets are assigned a value of 0% (or negligible), 50%, 75%, and 100% for particle lift.

The initial particle lift is an indicator that penetration could occur at an inconsistent penetration rate, particularly with coarse-grained sizes. Even the presence of particles beginning to cover the lower quarter of the droplet within the first few moments is indicative of an altered, interrupted penetration rate. The particle lift controls the WDPT on the coarse-grained material, due to the high volumetric ratio of the particles that are lifted to the droplet playing a bigger role in global changes in contact angles. Increasing hydrophobicity increases the lifting potential and forces at the surface of the droplet. Weak hydrophobicity in coarse soils does not have the lifting potential on the particles, suggesting that the overall process would be increasingly influenced. Lack of lifting and fully moving the individual particles at a higher degree of hydrophobicity, relative to one another, could produce a more pronounced conical shape bottleneck beneath the water droplet. While this event is inconsistent amongst trials, it does consistently appear within the dataset as a whole. This lower potential to fully move particles is due to the gravitational forces opposing the particle lift; even low hydrophobic levels contain some lift, but higher repellency rates show higher degrees of particle cover earlier in the penetration process. This is not as influential in the fine-grained samples due to the mass of the individual particles themselves, especially when directly compared to the coarse-grained material.

A particle that is lifted creates a new interface, and any interface is unstable. In addition, there is an additional dry surface to be wetted and air pockets underneath every lifted particle, creating unsaturated flow and hindering infiltration. Larger air pockets and dry surfaces to be wetted underneath larger lifted particles hinder the infiltration more.

Particle lift for the fine-grained material is less influential due to the localized (not global) contact angle change of smaller air pockets and the dry surface underneath smaller lifted particles. This is detailed qualitatively in Tables 2 and 3 and shown in Figures 10–13 by the lifting percentage on the face of the droplet, as well as quantitatively in the drop in sorptivity values between Regimes 1 and 2.

Table 2. The approximate coverage (opacity) ratio of lifted particles' volume for smooth infiltration at the moment of droplet placement (Regime 1).

Concentration (%) Grain Size	**0.6%**	**0.7%**	**0.8%**
Coarse	None	Low	None
Medium	Low	Low	Low
Fine	None	Mild	Mild

Table 3. The approximate coverage ratio of particle lifts' opacity volume for smooth infiltration at the first 0.5 mm of droplet penetration (Regime 2).

Concentration (%) Grain Size	**0.6%**	**0.7%**	**0.8%**
Coarse	Low	High	Low
Medium	Low	Mild	Mild
Fine	Low	Mild	Mild



(**a**) (**b**) (**c**)

Figure 11. Hydrophobic, fine-grained, 0.8% concentration Drop 9 (with faster penetration) at: (**a**) initial contact, (**b**) 3 s, and (**c**) 4 s later.



(**a**) (**b**) (**c**)

Figure 12. Hydrophobic, fine-grained, 0.8% concentration Drop 1 (with slower penetration) at: (**a**) initial contact, (**b**) 1 min, and (**c**) 5 min later.



Figure 13. Coarse grain, 0.7% concentration, Drops 2 and 1 from left to right with particle lift and reorientation at 5 and 8 s, respectively (i.e., grains protruding from the droplet marble, reorientating during penetration).

Particle lifts early in the WDPT can predict the interruption of infiltration by changing the expected rates (i.e., Regime 1) to disrupted rates (i.e., Regime 2). While this is particularly prevalent in the coarse-grained samples, it does not appear as governing in the fine samples with the same influence. The medium samples are affected by the particle lift, although not as strongly as seen in the fluctuation of the data. This could explain the unpredictability of the medium-grained sample results comparatively to the coarse- and fine-grained materials.

The results of the droplet height vs. time (Figures 1–3), appear to be segregated into separate classes. While not every class is visible in each dataset, the distinction can likely be attributed to particle lift. Different classes of infiltration resulting in segregated WDPT times in the coarse material could be due to the larger impact of the orientation of lifted particles on the contact angle hindering droplet penetration. The coarse-grained material consists of particles 0.6–2.0 mm in size, which is comparable with the average height of the droplets at the initial point of contact, which is approximately 2.6 mm. These larger particles are individually heavier, and particle lift—while observed in nearly every case at some point during the WDPT—rarely lifts particles fully off the original surface. This suggests that at this gradation size, the forces at the surface of the droplet lifting the grains are not strong enough to overcome the full gravitational force to dislodge the particles. The forces are, however, strong enough to reorientate particles and create a funnel or inverted cone-like shape in the soil bed, which would change the contact angle to one hindering droplet penetration. This can essentially create a moving bottleneck that interrupts the flow of droplet penetration. As discussed previously in the Section 2, more hydrophobic grains and grain faces will orientate themselves outward, creating a barrier for wetting and droplet penetration. This is supported by the current understanding of self-organization due to inconsistent hydrophobic coatings [8,25].

This alteration (i.e., creating a further barrier at or near the top air–water interface with lifted particles) is not observed in the fine-graded specimens to the same degree. This is likely due to the localized alteration of the contact angle on the surface of individually lifted fine particles and their inability to create a barrier to wetting. This suggests that larger grain sizes have masses and gravitational pulls that are approximately equivalent to or larger than the intrinsic forces at the surface of the water to reorganize the loose particles at the surface. The fine particles will self-organize, going through the same process as the coarse particles. The difference between the samples is the intrinsic lifting forces that are applied to these particles and ability to overcomee the gravitational pull based on individual particle mass. In other words, fine particles have left the soil surface and may or may not impact the droplet penetration into the soil surface.

The variation in the penetration time seen across test specimens with consistent gradations and induced hydrophobicity indicates more complex actions happening at the surface of the specimen than previously predicted. The entrance pressure required for the specimens should have remained reasonably constant; the droplet height vs. droplet

penetration time plots (Figures 1–3) show segregation in both penetration time and the rate of infiltration.

Regime 1 is referred to when the slope of Figures 1–3 is steeper, representing a consistent rate of infiltration through the middle 80% of the full WDPT time, observed in most test specimens. This is when the particle lift effect is minimal, e.g., minimum particle lifts in coarse samples and fine samples in general. If Regime 1 is the only observed regime, the case is referred to as 'Uninterrupted.'

Regime 2 is referred to when the slope of Figures 1–3 or Figures 4–6 is shallower, representing slower droplet penetration and higher infiltration time. This is observed when the particle lift impact is considerable, e.g., considerable particle lifts in coarse samples. Regardless of the existence of Regime 1, if Regime 2 occurs, there is a delay in droplet penetration due to particle lift. The case is then referred to as having an 'Interrupted' rate of change, where the WDPT can be categorized as having an expected larger value. This near-constant rate is consistent with the existing literature and currently accepted models of unsaturated flow. The large deviation from the uninterrupted (Regime 1) predicted rate will be referred to as 'Interrupted' here on.

The uninterrupted case, in turn, produces lower-than-expected sorptivity values when compared with the remainder of the interrupted samples with larger sorptivity values. As mentioned, a combination of Regimes 1 and 2 is also seen in a stair-stepping-like, considered 'interrupted', infiltration rate. When Figures 2–4 are fitted to a third-order polynomial line, shown in Figures 14–16, these interrupted samples can be classified as infiltration plots with an inflection point in the middle portion of the plot. These fitted graphs smooth and exaggerate the curvature of the infiltration process and magnify the key discrepancies that separate the two regimes. Figures 14–16 were only utilized to separate the interrupted and uninterrupted infiltration and show a processed version of Figures 2–4 (see the Supporting Documents for the equations and standard deviations of these trendlines). The middle portion of the infiltration is essentially caused by a barrier effect or retardation of the droplet penetration seen as rapid penetration (i.e., Regime 1), which is followed by delayed penetration (i.e., Regime 2) and then rapid penetration (i.e., Regime 1). This observation became more pronounced when the plots were converted into best-fit polynomials (see Figure 14a for coarse, 0.6% surrogate dilution, and the purple trendlines for Drops 1, 3, and 6, ending between 1200 and 2100 s).

Under normal circumstances, a decrease in grain size from the coarse-grained to fine-grained range of poorly graded (specifically uniform) porous media is expected to correspond to a longer infiltration time. In finer-grained soils, as the specific surface area increases and pore diameter decreases, the infiltration rate is expected to decrease in both saturated and unsaturated flow, resulting in increased WDP time. An increase in the pore sizes in coarse-grained soils is expected to increase the infiltration rate and decrease the infiltration time. However, this expectation does not account for particle lift. When particles are lifted, the surface roughness artificially increases, and the uniform contact angles expected on a smooth surface are tilted. This tilt can be localized on the surface of fine-grained soils or be more pronounced on the surface of large-grained soils. This alteration of the contact angle can induce more instability in the expected droplet penetration. Hence, two clear regimes are expected to govern the droplet penetration into coarse materials—Regime 1 when no particle lift occurs (no delayed WDP) and Regime 2 for cases when a particle lift occurs and there is more delayed WDP. This is the key trigger for the creation of the two regimes to differentiate between the aforementioned findings and the general blanket statement of a higher classification of hydrophobicity, as seen in all research that utilizes the WDPT.

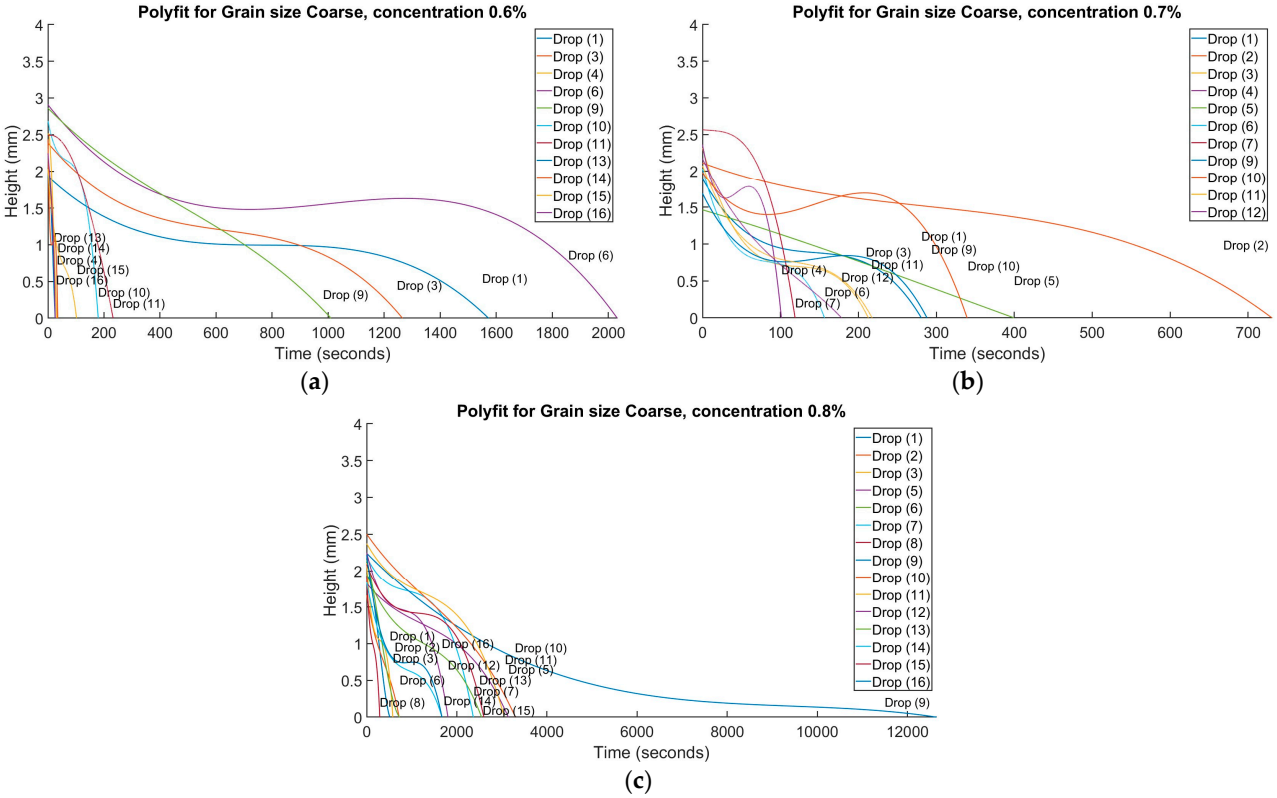


Figure 14. Water Droplet Penetration Test best-fit third-order polynomial (i.e., height vs. time) for coarse-grained soil for hydrophobicity-inducing surrogate dilutions of (**a**) 0.6%, (**b**) 0.7%, and (**c**) 0.8%.

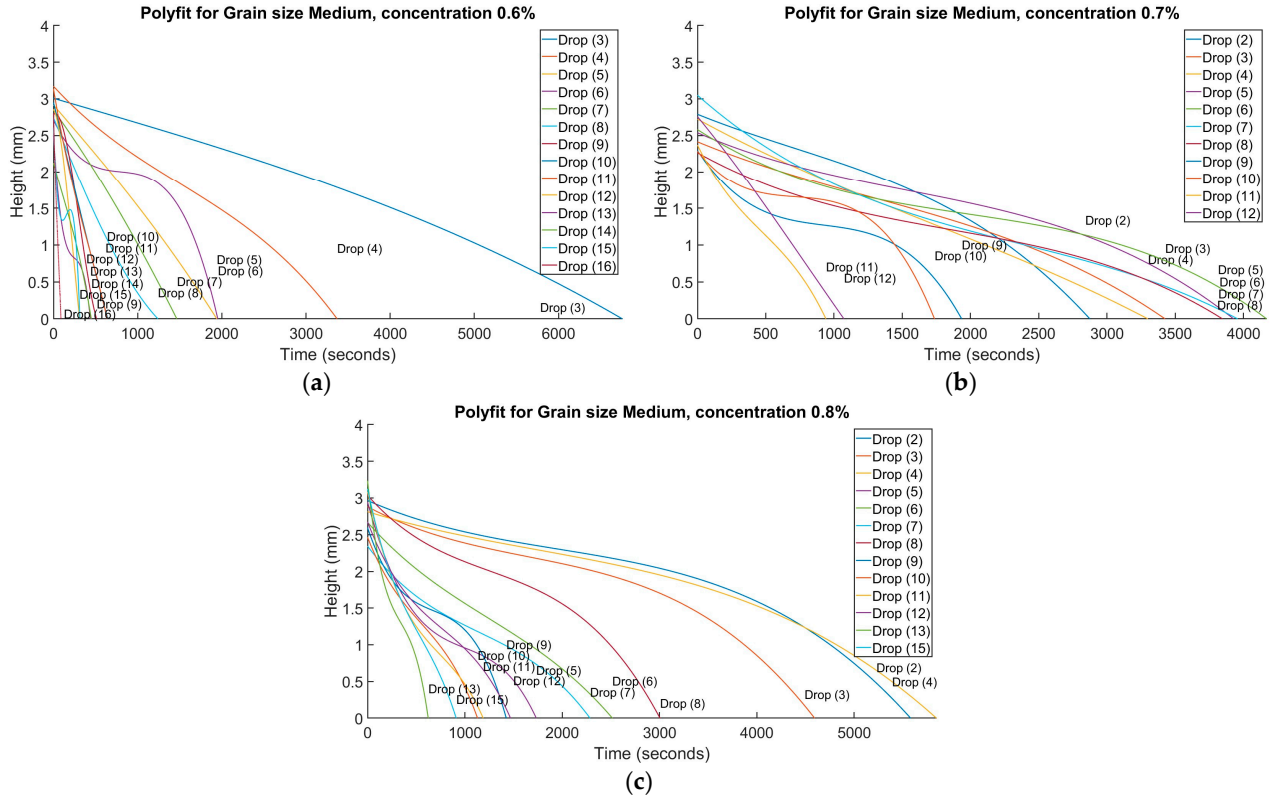


Figure 15. Water Droplet Penetration Test best-fit third-order polynomial (i.e., height vs. time) for medium-grained soil for hydrophobicity-inducing surrogate dilutions of (**a**) 0.6%, (**b**) 0.7%, and (**c**) 0.8%.

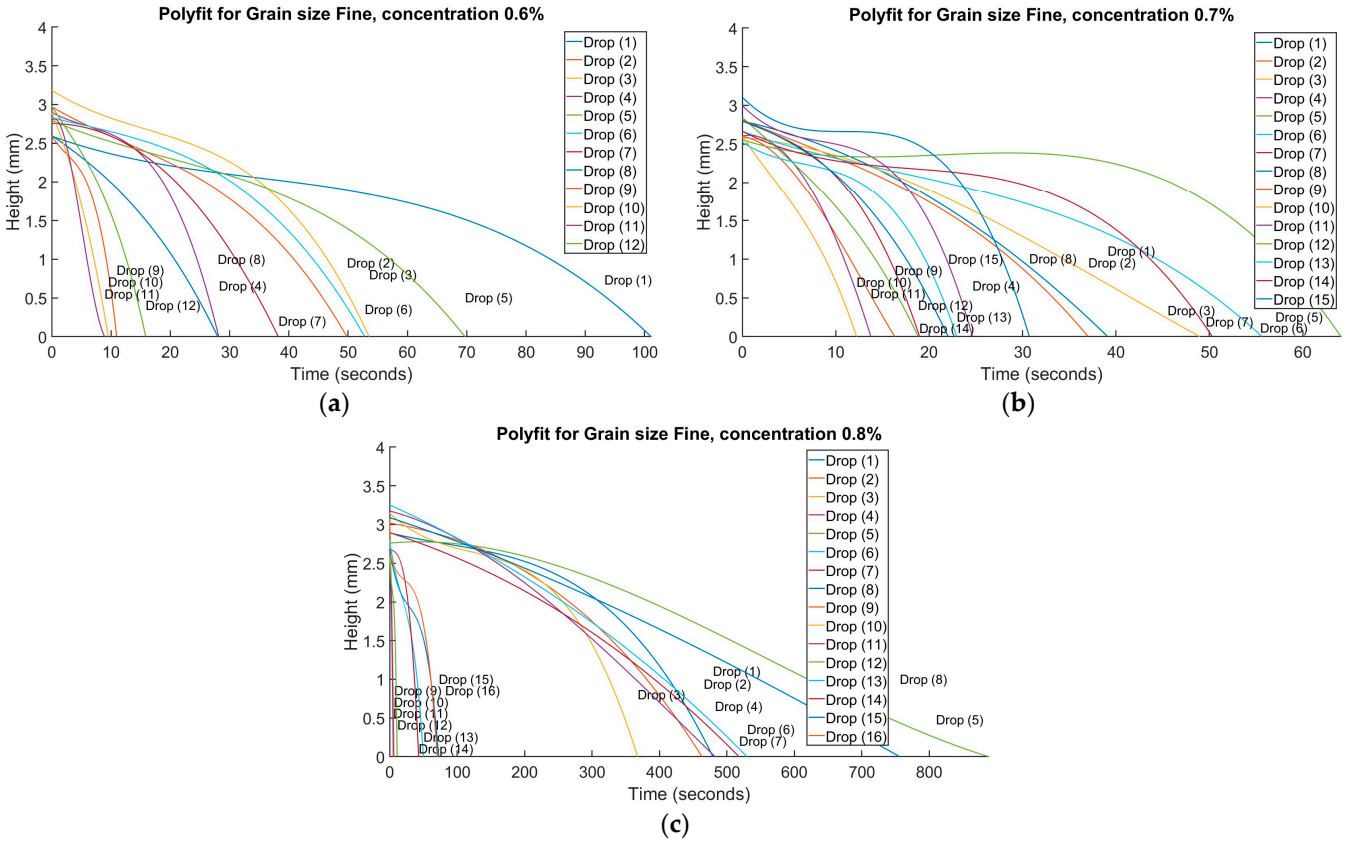


Figure 16. Water Droplet Penetration Test best-fit third-order polynomial (i.e., height vs. time) for fine-grained soil for hydrophobicity-inducing surrogate dilutions of (**a**) 0.6%, (**b**) 0.7%, and (**c**) 0.8%.

As mentioned, the WDPT is longer for coarse hydrophobic soils when particle lift happens, while the WDPT is shorter for finer soils. With the exception of the 0.7% dilution for the fine-grained samples, this faster trend of infiltration rates for the WDPT is observed. The fine-grained sample (0.3 mm nominal size) showed faster infiltration rates, by approximately one order of magnitude, than the medium and coarse samples.

This contradicts the presumed order based on the grain size and the well-established understanding of saturated seepage through porous media. However, the justification for this behavior is the impact of particle lift. Smaller solid particles can easily lift but cannot alter the contact angle and, in turn, hinder the penetration and alter time. However, coarser particles attracted to the surface of the droplet occupy and alter a much larger portion of the volume of the droplet, as well as alter the penetration.

The control samples appeared fully wettable and hydrophilic. When monitored using the digital camera, recording one image every 0.017 s, both the coarse and medium samples showed droplets fully infiltrated within 0.1 s and never formed a water marble or stable shape on top of the test specimens. The fine samples had all droplets fully infiltrated with an average of 0.127 s. For hydrophilic coarse-grained soils with extremely fast droplet penetration (i.e., much shorter droplet penetration time), the two regimes may not be distinctly visible. However, for the slow droplet penetration (i.e., longer droplet penetration time), the difference between the two regimes is more visible.

Hence, coarse-grained samples across all surrogate dilutions show more distinct regimes; i.e., Regime 2 shows a much longer WPD time. The WDPT also increases as the hydrophobicity increases, and the difference between the WDPT for cases of only Regime 1 and those of Regime 2 (i.e., Regime 2 alone, or Regimes 1 and 2) increases as well. An outlying data point, Drop 2 (for the coarse sample at 0.7% surrogate dilution), would fully penetrate at approximately 1110 s if linearly extrapolated comparatively to the range of

100–400 s for all other drops. Both regimes were observed in all WDPT trials for all grain sizes and surrogate concentrations.

Upon examining the observations across all droplets and cases, the average ranges of WDPT times are shown above in Table 1. The drops were then separated based on infiltration characteristics. This included only the following two scenarios: when only Regime 1 was observed, referred to as 'uninterrupted' by particle lift, and when Regime 2 was also observed, referred to as 'interrupted' by particle lift. Interrupted infiltration includes Regime 2, regardless of the existence of Regime 1, but uninterrupted infiltration includes only Regime 1—without Regime 2. These calculations were based on the full time to WDP, aligning with the digital imaging of particle lifts in droplets. Tables 2 and 3 display the opacity of droplet images, which represent particle lift, which corresponds to the occurrence of Regime 2 in interrupted infiltration.

The number, n, and standard deviation, s, in (s) values in Figure 17a are n = 5 and s = 58.132 for 0.6% dilution, n = 5 and s = 47.980 for 0.7% dilution, and n = 4 and s = 183.969 for 0.8% dilution. The values of n and s for Figure 17b are n = 7 and s = 184.966 for 0.6% dilution, n = 2 and s = 56.615 for 0.7% dilution, and n = 5 and s = 383.334 for 0.8% dilution. The values of n and s are n = 4 and s = 2.700 for 0.6% dilution, n = 8 and s = 5.563 for 0.7% dilution, and n = 4 and s = 2.320 for 0.8% dilution.

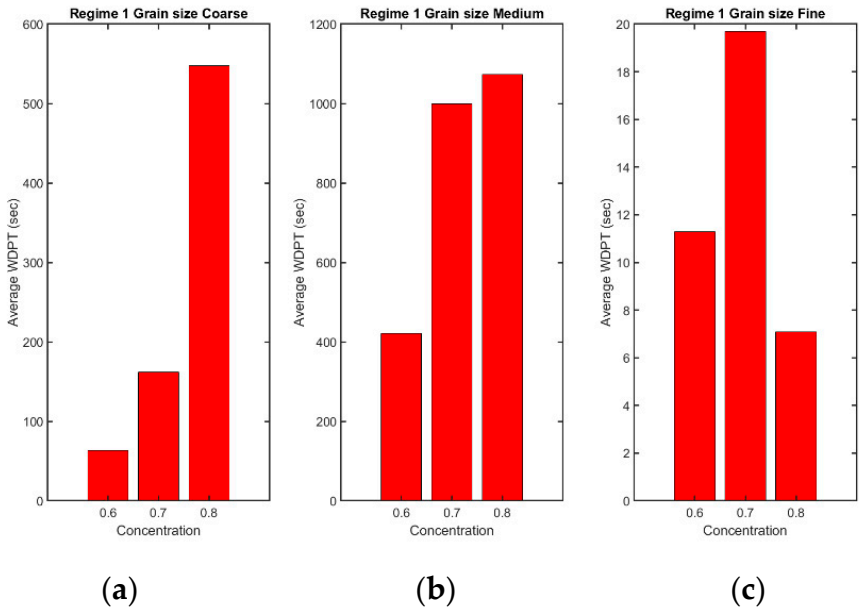


Figure 17. Average Water Droplet Penetration Test values for uninterrupted infiltration cases (Regime 1 only) across all specimens inducing surrogate dilutions of (**a**) 0.6%, (**b**) 0.7%, and (**c**) 0.8%.

The number, n, and standard deviations, s, in (s) for Figure 18a are n = 5 and s = 846.165 for 0.6% dilution, n = 4 and s = 46.767 for 0.7% dilution, and n = 2 and s = 400.900 for 0.8% dilution. For Figure 18b, the values of n and s are n = 6 and s = 840.364 for 0.6% dilution, n = 2 and s = 141.9 for 0.7% dilution, and n = 5 and s = 689.570 for 0.8% dilution. The values of n and s for Figure 18c are n = 7 and s = 21.740 for 0.6% dilution, n = 7 and s = 12.081 for 0.7% dilution, and n = 10 and s = 247.889 for 0.8% dilution.

Tables 4 and 5 above show the exact values graphically shown in Figures 17 and 18. The average values shown are obtained from the extrapolated data seen in Figures 14–16. When the standard deviation values between Figures 17 and 18 are compared, the general upward trend is approximately double in most cases. The sporadic behavior of the interrupted Regime 2, caused by particle lifting, is reflected in this analysis.

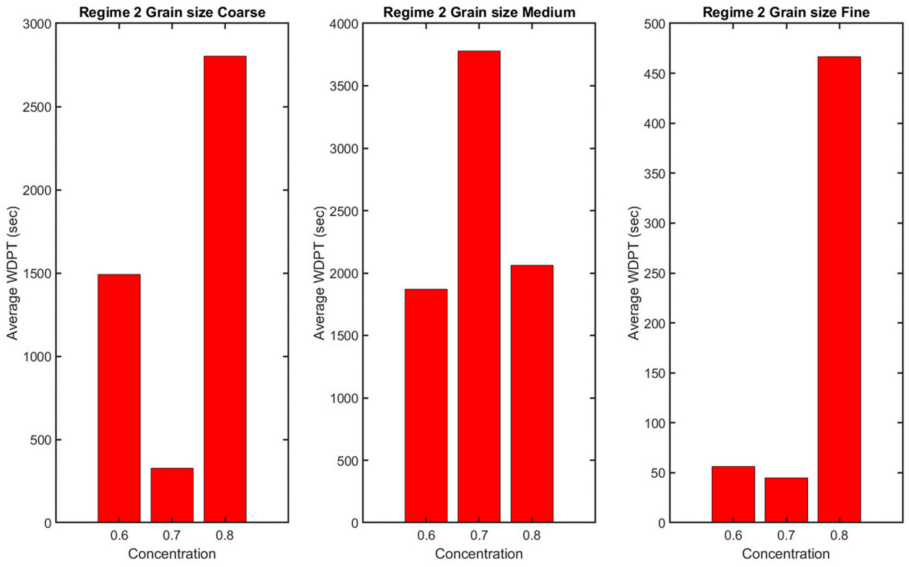


Figure 18. Average Water Droplet Penetration Test values for interrupted infiltration cases (Regime 2 exists) across all specimens inducing surrogate dilutions of (**a**) 0.6%, (**b**) 0.7%, and (**c**) 0.8%.

Table 4. WDPT (s) for the uninterrupted infiltration (Regime 1 alone).

Concentration (%) Grain Size	**0.6%**	**0.7%**	**0.8%**
Coarse	63.4	162.3	547.5
Medium	421.8	999.3	1072.9
Fine	11.3	19.7	7.1

Table 5. WDPT (s) for the Interrupted infiltration (Regime 2 was also observed).

Concentration (%) Grain Size	**0.6%**	**0.7%**	**0.8%**
Coarse	1490.6	327.1	2802.2
Medium	1868.8	3779.5	2061.7
Fine	56.0	44.8	466.4

The WDPT values separated for uninterrupted (Regime 1 alone), and interrupted (Regime 2) infiltration cases were used to calculate the sorptivity using Equation (2) for all grain sizes and surrogate dilutions for up to 16 replicated drops. The entire sorptivity results are shown in Figures 17 and 18. Tables 6 and 7 also show the average sorptivity for grain sizes and surrogate dilution levels for all drops grouped in two uninterrupted and interrupted classes. These tables show the data points visually represented by the green and red lines seen in Figures 19–21.

Table 6. Average sorptivity ($mm/s^{0.5}$) values of uninterrupted infiltration (Regime 1 alone).

Concentration (%) Grain Size	0.6%	0.7%	0.8%
Coarse	2.53	1.43	0.48
Medium	1.45	0.56	0.94
Fine	7.23	5.77	7.51

Table 7. Average sorptivity ($mm/s^{0.5}$) values of interrupted infiltration (Regime 2 occurs).

Concentration (%) Grain Size	0.6%	0.7%	0.8%
Coarse	0.62	0.77	0.21
Medium	0.63	0.29	0.49
Fine	3.57	3.41	1.61

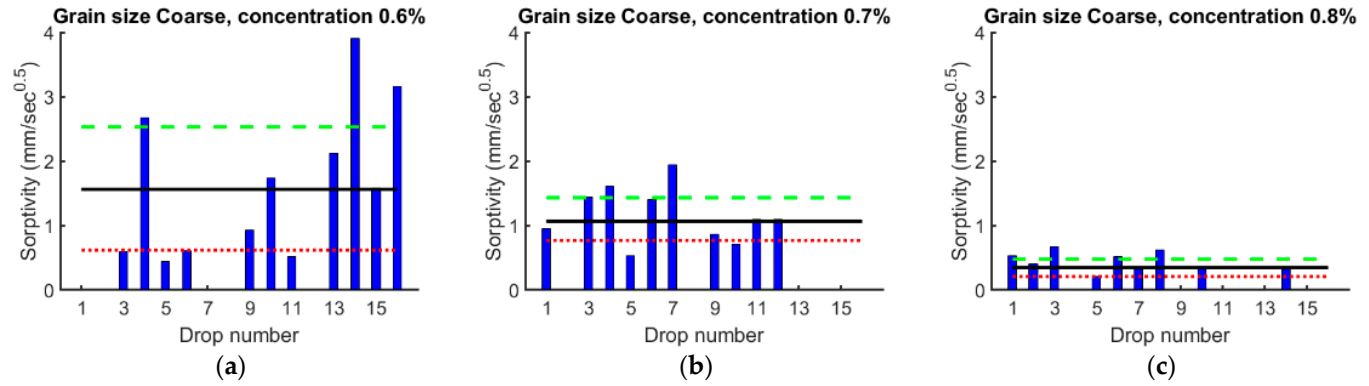


Figure 19. Calculated sorptivity values for each droplet that was observed through the full penetration time for the coarse-grained soil for hydrophobicity-inducing surrogate dilutions of (**a**) 0.6%, (**b**) 0.7%, and (**c**) 0.8%. Red and green dashed lines mark the average of cases with interrupted and uninterrupted infiltration by particle lift with slower and faster WDP, respectively.

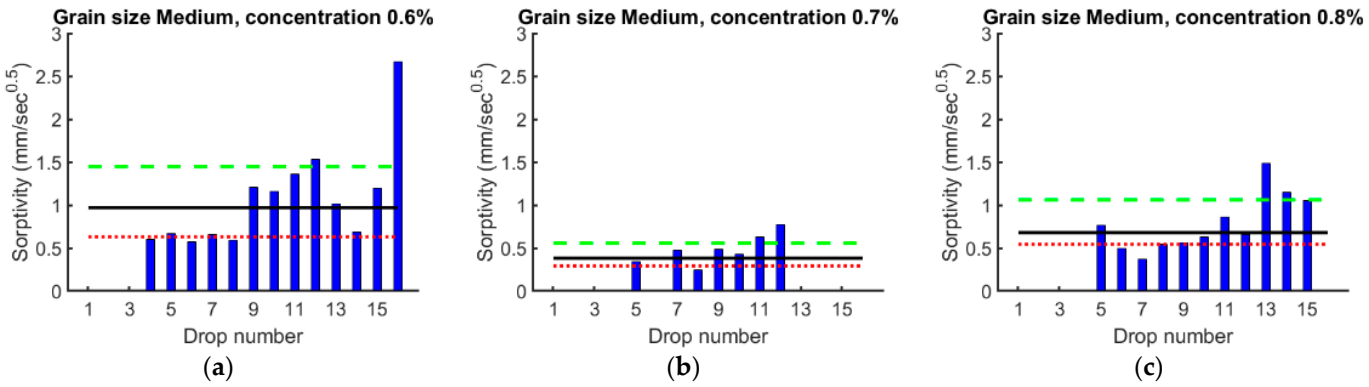


Figure 20. Calculated sorptivity values for each droplet that was observed through the full penetration time for the medium-grained soil for hydrophobicity-inducing surrogate dilutions of (**a**) 0.6%, (**b**) 0.7%, and (**c**) 0.8%. Red and green dashed lines mark the average of cases with interrupted and uninterrupted infiltration by particle lift with slower and faster WDP, respectively.

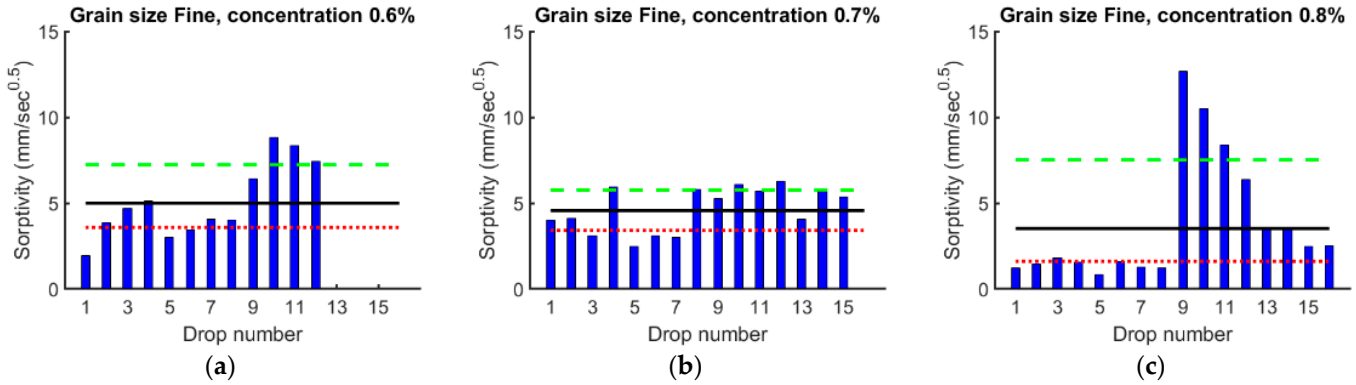


Figure 21. Calculated sorptivity values for each droplet that was observed through the full penetration time for the fine-grained soil for hydrophobicity-inducing surrogate dilutions of (**a**) 0.6%, (**b**) 0.7%, and (**c**) 0.8%. Red and green dashed lines mark the average of cases with interrupted and uninterrupted infiltration by particle lift with slower and faster WDP, respectively.

The solid line in each sorptivity plot of Figures 19–21 marks the average value across all calculated sorptivity values for all drops, and the red and green dashed lines line show the average for drops grouped into uninterrupted and interrupted by particle lift, respectively. These figures show a discernible trend of decreasing sorptivity with the increase in hydrophobicity induced by the increase in surrogate concentration in all cases as a general trend, as expected. The presence of any hydrophobic compound that reduces the soils' ability to absorb water can be attributed to the interaction between the hydrophobic compounds within the surrogate and the water, decreasing sorptivity and hindering droplet penetration. The outliers, as seen in the medium-grained samples, were likely skewed by the penetration mechanism distinguishing the interrupted regime at the boundary of the critical influence of grain size and particle weight. The altered wettability can be seen in both the sorptivity (Figures 17–21), and the contact angle plots (Figures 5–7).

Figures 19–21 show the calculated sorptivity values of each drop that achieved full penetration during the observation period. The top green line is the average of Regime 1 alone with smooth uninterrupted infiltration. The black solid line in the middle is the divider between the uninterrupted and interrupted infiltration. The red and green lines show the average of the interrupted and uninterrupted infiltration cases.

4.2. Discussion

The absolute values in Figures 19–21 show that coarse grains at higher hydrophobicity (0.8% surrogate concentration) show the same behavior and sorptivity values as medium grains at intermediate hydrophobicity (0.7% surrogate concentration) and fine grains at lower hydrophobicity (0.6% surrogate concentration). This is consistent with expected delayed infiltration in finer soils. This also demonstrates the fact that WDPT results can only be used for general SWR levels without consideration of the soil grain size and emphasizes the need to calibrate WDPT results based on the soil grain size for any higher-level analysis.

The effect of hydrophobic surrogate dilution is more pronounced in the coarse-grained samples than in the medium- and fine-grained samples. The fine-grained samples, having an overall faster infiltration rate, as seen in Figures 2 and 5 when comparing coarse- and fine-grained samples at the same concentrations, is most severe. This is even more pronounced because when the same quantity of hydrophobicity-inducing surrogate is added to the fine-grained samples with a higher specific surface area (SSA) for a similar mass, more hydrophobicity and longer WDP time and smaller sorptivity values are expected than in the coarse-grained sample, which is against observations of Figures 2 and 5. This observation confirms the need for calibrating the WDPT to various grain sizes.

For a given grain size, any increase in hydrophobicity should generally increase the WDPT and decrease sorptivity within each class of interrupted or uninterrupted infiltration,

which is also observed here. Environmental influences, while consistent across all tests, could influence the grain size and concentration. This indicates that both the physical properties of the soil surface, the degree of hydrophobicity, and the properties of the water play significant roles in the WDPT results.

The fine-grained sorptivity samples, in Figure 21 and in Tables 6 and 7, show an anomaly in Drops 9 through 12 for infiltration speed and calculated sorptivity values. The droplets within the second regime follow the same logical trend of decreased sorptivity, or increased WDP time. The rapid infiltration of Drops 9 through 12 is outside of the expected range and outside of the expected experimental margin of error. This is an area that would need future investigation.

As seen in the penetration time shown in Figures 2–7, and sorptivity averages shown in Figures 8 and 9, the results are erratic and follow no obvious pattern. However, the correlation of the occurrence of particle lift, seen in droplet images of Figures 11–13 with similarities in values for the penetration time and sorptivity results divided into two groups, supports the existence of two distinct regimes. The separation of the two regimes is even more obvious in poly-fitted curves of Figures 14–16. The evidence of these two regimes can directly highlight some of the subjectivity and inaccuracies of the WDPT methodology, even when consistent specimens are provided. Regime 1 with minimal particle lift and Regime 2 with considerable particle lift delaying droplet penetration are found to be the primary mechanisms responsible for creating sporadic results. The appearance of Regime 2, especially in coarse-grained soils, caused more apparent delays in infiltration and smaller sorptivity (Figure 14). The distinction of the two regimes is as visible in the fine-grained case at 0.8% concentration (Figure 16c). The relation between the delayed infiltration and decreased sorptivity was studied here across soil grain size and level of hydrophobicity through additional dimensions of measurement with the WDPT. The reduced sorptivity was hypothesized when SWR was increased; however, the predictability of sporadic results based on the appearance of particle lift proved telling. These observations highlight the need for the further development of calibrations to the WDPT method, in addition to findings of the particle lift's impacts on infiltration in hydrophobic sands.

The combination of results across grain sizes, sorptivity, and observed particle lift clearly demonstrates the potential for new additions to the WDPT. The methodology provided by Letey at test conception [6], as well as past and current research utilizing the test since conception, are not invalidated by these findings. These findings highlight the subjectivity of the included results and why this method is typically used in conjunction with additional methods. A comparison of WDPT classification against sorptivity alone as an indicator of SWR without considering the distinct regimes is likely fallible unless additional dimensions of measurement are utilized. Particle lift evaluations are an example of one such dimension. Similarly, particle lift against sorptivity can be utilized in a population of data to show regime but is likely fallible as a sole source for WDPT classification. The additional dimensions of examination to show data segregation by regime studied here, or other dimensions for investigation to be included or developed, is required for a full material and property analysis of hydrophobic soils.

5. Conclusions

The Water Droplet Penetration Test is widely utilized to identify water-repellent soils. The subjectivity of the test when used for purposes outside of general classification is, however, exacerbated when differing site conditions, environmental factors, grain sizes, and soil types are tested unilaterally. New test methods, as well as existing test procedures not commonly used, are becoming more frequently utilized. These methods used to identify and classify SWR come from methods without the ability to correlate, correct, or calibrate to specific conditions. The analysis and understanding of these impacts—which helps to calibrate the WDPT—enable this basic testing procedure to be increasingly uniform across all types and conditions of soil and allow for a higher precision of comparison between independent research projects. The inclusion of correlation, correction, or calibration factors

could be utilized to improve the WDPT method, and the findings in this paper may set the groundwork for these factors.

This paper investigates the impact of various levels of hydrophobicity on soil samples of various grain sizes. It also investigates the impact of lifted hydrophobic particles on delaying water droplet infiltration across soil grain size and hydrophobicity level. The importance of particle lift in coarser soils and the variation in this importance with increasing hydrophobicity was also studied and demonstrated. This observation not only shows the importance of a calibration factor for the WDPT methodology but also the appearance of two distinctive regimes. These regimes have likely been overlooked in prior works and marked as higher classifications of SWR. This is not an incorrect assessment of the soil, although it does not speak to the actual mechanisms and other properties of the material. Hydrophobicity-induced particle lift causes instability (i.e., chaotic, and inconsistent lifting of some particles and not others), leading to two distinct regimes that seem to randomly occur. However, like most instabilities in nature, they are deterministic and a function of soil heterogeneity (various grain sizes and shapes) and nonuniform hydrophobic coating.

The experimentation in this work was limited by manual measurements of height and contact angles, as well as the methodology utilized to calculate sorptivity. Specialized equipment utilized to continuously monitor water marble volumetrics, in addition to surface tension, experimentally determined sorptivity, and modeling of the particle lifting phenomenon would further support these findings.

Additional research is needed to better understand the processes highlighted here to illustrate the impactful mechanisms found. Future works can include a finer quantitative analysis of particle lift and its correlation to the infiltration rate, as well as find ways to predict whether particle lift will occur or not for a certain case. As mentioned, a higher magnitude of particle lift interrupts the droplet penetration more, which, in turn, delays infiltration and decreases sorptivity. However, the development of this correlation could be quantitatively performed with minor alterations to the presented methodology with the inclusion of additional specialized testing. Additional work in calibrating the WDPT to grain size can also further this work, particularly after a correlation is produced with sorptivity.

Supplementary Materials: The following supporting information can be downloaded at: https://www.mdpi.com/article/10.3390/geotechnics4020032/s1.

Author Contributions: Conceptualization, M.V. and A.F.; methodology, M.V.; software, M.V. and A.F.; validation, M.V.; formal analysis, M.V. and A.F.; investigation, M.V.; resources, M.V.; data curation, M.V.; writing—original draft preparation, M.V.; writing—review and editing, M.V. and A.F.; visualization, M.V.; supervision, A.F.; project administration, A.F.; funding acquisition, A.F. All authors have read and agreed to the published version of the manuscript.

Funding: This research was funded by the National Science Foundation, NSF, through the DUE Program, Award No. 1930464.

Data Availability Statement: The data presented in this study are openly available in article.

Conflicts of Interest: The authors declare no conflict of interest.

References

1. Granged, A.J.P.; Zavala, L.M.; Jordán, A.; Bárcenas-Moreno, G. Post-Fire Evolution of Soil Properties and Vegetation Cover in a Mediterranean Heathland after Experimental Burning: A 3-Year Study. *Geoderma* **2011**, *164*, 85–94. [CrossRef]
2. Mataix-Solera, J.; Doerr, S.H. Hydrophobicity and Aggregate Stability in Calcareous Topsoils from Fire-Affected Pine Forests in Southeastern Spain. *Geoderma* **2004**, *118*, 77–88. [CrossRef]
3. Newland, J.A.; DeLuca, T.H. Influence of Fire on Native Nitrogen-Fixing Plants and Soil Nitrogen Status in Ponderosa Pine—Douglas-Fir Forests in Western Montana. *Can. J. For. Res.* **2000**, *30*, 9. [CrossRef]
4. Parson, A.; Robichaud, P.R.; Lewis, S.A.; Napper, C.; Clark, J.T. *Field Guide for Mapping Post-Fire Soil Burn Severity*; US Department of Agriculture, Forest Service, Rocky Mountain Research Station: Fort Collins, CO, USA, 2010; p. RMRS-GTR-243.

5. Robichaud, P.R.; Lewis, S.A.; Ashmun, L.E. *New Procedure for Sampling Infiltration to Assess Post-Fire Soil Water Repellency*; US Department of Agriculture, Forest Service, Rocky Mountain Research Station: Fort Collins, CO, USA, 2008; p. RMRS-RN-33.
6. Letey, J. Measurement of contact angle, water drop penetration time, and critical surface tension. In *Water-Repellent Soils: Proceedings of the Symposium on Water-Repellent Soils, Riverside, CA, USA, 6–10 May 1968*; DeBano, L.F., Letey, J., Eds.; University of California: Riverside, CA, USA, 1969; pp. 43–47.
7. Letey, J.; Carrillo, M.L.K.; Pang, X.P. Approaches to Characterize the Degree of Water Repellency. *J. Hydrol.* **2000**, *231–232*, 61–65. [CrossRef]
8. McHale, G.; Shirtcliffe, N.J.; Newton, M.I.; Pyatt, F.B.; Doerr, S.H. Self-Organization of Hydrophobic Soil and Granular Surfaces. *Appl. Phys. Lett.* **2007**, *90*, 054110. [CrossRef]
9. Shillito, R.M. *Infiltration into Water-Repellent Sand: The Role of Sorptivity*; University of Nevada: Las Vegas, NV, USA, 2020.
10. DeBano, L.F. The Role of Fire and Soil Heating on Water Repellency in Wildland Environments: A Review. *J. Hydrol.* **2000**, *231–232*, 195–206. [CrossRef]
11. Letey, J.; Osborn, J.; Pelishek, R.E. The Influence of the Water-Solid Contact Angle on Water Movement in Soil. *Int. Assoc. Sci. Hydrol. Bull.* **1962**, *7*, 75–81. [CrossRef]
12. Huffman, E.L.; MacDonald, L.H.; Stednick, J.D. Strength and Persistence of Fire-Induced Soil Hydrophobicity under Ponderosa and Lodgepole Pine, Colorado Front Range. *Hydrol. Process.* **2001**, *15*, 2877–2892. [CrossRef]
13. Steenhuis, T.S.; Hunt, A.G.; Parlange, J.-Y.; Ewing, R.P. Assessment of the Application of Percolation Theory to a Water Repellent Soil. *Soil Res.* **2005**, *43*, 357. [CrossRef]
14. Zavala, L.M.; González, F.A.; Jordán, A. Intensity and Persistence of Water Repellency in Relation to Vegetation Types and Soil Parameters in Mediterranean SW Spain. *Geoderma* **2009**, *152*, 361–374. [CrossRef]
15. Pardini, G.; Gispert, M.; Dunjo, G. Relative Influence of Wildfire on Soil Properties and Erosion Processes in Different Mediterranean Environments in NE Spain. *Sci. Total Environ.* **2004**, *328*, 237–246. [CrossRef] [PubMed]
16. Carballeira, A. Phenolic Inhibitors in *Erica australis* L. and in Associated Soil. *J. Chem. Ecol.* **1980**, *6*, 593–596. [CrossRef]
17. Ammar, H.; López, S.; González, J.; Ranilla, M.J. Correlation between Analytical and Biological Techniques for the Assessment of Phenolic Compounds in Spanish Browse Species. Available online: https://om.ciheam.org/article.php?IDPDF=4600174 (accessed on 15 April 2024).
18. Doerr, S.H.; Shakesby, R.A.; Walsh, R.P.D. Soil Water Repellency: Its Causes, Characteristics, and Hydro-Geomorphological Significance. *Earth-Sci. Rev.* **2000**, *51*, 33–65. [CrossRef]
19. DeBano, L.F.; Rice, R.M.; Conrad, C.E. *Soil Heating in Chaparral Fires: Effects on Soil Properties, Plant Nutrients, Erosion, and Runoff*; Department of Agriculture, Forest Service, Pacific Southwest Forest and Range Experiment Station: Berkeley, CA, USA, 1979; 21p.
20. Ngole-Jeme, V.M. Fire-Induced Changes in Soil and Implications on Soil Sorption Capacity and Remediation Methods. *Appl. Sci.* **2019**, *9*, 3447. [CrossRef]
21. MacDonald, L.H.; Huffman, E.L. Post-Fire Soil Water Repellency: Persistence and Soil Moisture Thresholds. *Soil Sci. Soc. Am. J.* **2004**, *68*, 6. [CrossRef]
22. Zhang, C.; Liu, Z.; Deng, P. Contact Angle of Soil Minerals: A Molecular Dynamics Study. *Comput. Geotech.* **2016**, *75*, 48–56. [CrossRef]
23. Dyrness, C. *Effect of Wildfire on Soil Wettability in the High Cascades*; US Department of Agriculture, Forest Service, Pacific Northwest Forest and Range Experiment Station: Portland, OR, USA, 1976.
24. Campbell, R.E.; Baker, M.B.; Ffolliott, P.F.; Larson, F.R.; Avery, C.C. *Wildfire Effects on a Ponderosa Pine Ecosystem: An Arizona Case Study*; US Department of Agriculture, Forest Service, Rocky Mountain Forest and Range Experimental Station: Fort Collins, CO, USA, 1977; p. RM-191.
25. Doerr, S.H.; Thomas, A.D. The Role of Soil Moisture in Controlling Water Repellency: New Evidence from Forest Soils in Portugal. *J. Hydrol.* **2000**, *231–232*, 134–147. [CrossRef]
26. Philip, J.R. The theory of Infiltration: 4. Sorptivity and algebraic infiltration equations. *Soil Sci.* **1957**, *84*, 257–264. [CrossRef]
27. Bach, L.B.; Wierenga, P.J.; Ward, T.J. Estimation of the Philip Infiltration Parameters from Rainfall Simulation Data. *Soil Sci. Soc. Am. J.* **1986**, *50*, 1319–1323. [CrossRef]
28. Pazira, E. Studying the Philip Model Capability to Estimate Water Infiltration Parameters. In Proceedings of the 19th World Congress of Soil Science, Brisbane, Australia, 1–6 August 2010.

Disclaimer/Publisher's Note: The statements, opinions and data contained in all publications are solely those of the individual author(s) and contributor(s) and not of MDPI and/or the editor(s). MDPI and/or the editor(s) disclaim responsibility for any injury to people or property resulting from any ideas, methods, instructions or products referred to in the content.